

- described by P. Burchill and M. G. H. Wallbridge, *Inorg. Nucl. Chem. Lett.*, **12**, 93 (1976), but no characterization has been reported. All our attempts to obtain the same complexes following the experimental procedure described in the above paper were unsuccessful.
- (7) (a) R. L. Peksok and W. P. Scafer, *J. Am. Chem. Soc.*, **83**, 62 (1961); (b) H. J. Seifert and B. Gerstemberg, *Z. Anorg. Allg. Chem.*, **315**, 56 (1962).
 - (8) (a) F. Mani and G. Scapacci, *Inorg. Chim. Acta*, **16**, 163 (1976); (b) L. F. Larkworthy, K. C. Patel, and J. K. Trigg, *J. Chem. Soc.*, 2766 (1971).
 - (9) I. Bertini and F. Mani, *Inorg. Chem.*, **6**, 2032 (1967).
 - (10) "Philips Serving Science and Industry", No. 2, 18 (1972).
 - (11) C. Mealli, S. Midollini, and L. Sacconi, *Inorg. Chem.*, **14**, 2513 (1975).
 - (12) C. J. Ballhausen, "Introduction to Ligand Field Theory", McGraw-Hill, New York, N.Y., 1962.
 - (13) E. König, *Inorg. Chem.*, **10**, 2633 (1971).
 - (14) F. Mani, *Inorg. Nucl. Chem. Lett.*, **12**, 271 (1976).
 - (15) (a) H. M. Echols and D. Dennis, *Acta Crystallogr., Sect. B*, **30**, 2173 (1974); (b) D. F. Rendle, A. Storr, and J. Trotter, *J. Chem. Soc., Dalton Trans.*, 176 (1975); (c) D. J. Patmore, D. F. Rendle, A. Storr, and J. Trotter, *ibid.*, 718 (1975).
 - (16) D. C. Bradley, M. B. Hursthouse, C. W. Newing, and A. J. Welch, *J. Chem. Soc., Chem. Commun.*, 567 (1972).
 - (17) D. J. Brauer and C. Kruger, *Cryst. Struct. Commun.*, **3**, 421 (1973).
 - (18) J. P. Fackler, *Prog. Inorg. Chem.*, **7**, 361 (1966).
 - (19) F. A. Cotton and G. Wilkinson, "Advanced Inorganic Chemistry", 3rd ed., Interscience, New York, N.Y., 1972, p 630.
 - (20) M. R. Churchill, K. Gold, and C. E. Maw, Jr., *Inorg. Chem.*, **9**, 1597 (1970).
 - (21) F. A. Cotton, C. E. Rice, and G. W. Rice, *Inorg. Chim. Acta*, **24**, 231 (1977).
 - (22) D. H. Gerloch and R. H. Holm, *Inorg. Chem.*, **8**, 2292 (1969).

Contribution from the Departments of Chemistry, Texas A&M University, College Station, Texas 77843, and Princeton University, Princeton, New Jersey 08540

Molecular and Electronic Structure of Tetrakis(dimethylamido)molybdenum(IV)

MALCOLM H. CHISHOLM,^{1a} F. ALBERT COTTON,*^{1b} and MICHAEL W. EXTINE^{1b}

Received November 3, 1977

The molecular structure of Mo(NMe₂)₄ has been determined by x-ray crystallography and used to interpret the available data pertaining to the electronic structure of the molecule. The structure possesses virtual *D*_{2d} symmetry with the C–N–C planes perpendicular to the vertical symmetry plane of the *D*_{2d} point group. Both a qualitative symmetry analysis and a Hartree–Fock calculation in the Fenske–Hall approximation led to the conclusion that the two molybdenum 4d electrons should occupy the b₁ (*x*² – *y*²) orbital to give a singlet ground state, as observed, with the ordering of the empty d orbitals being z², (*xz*, *yz*), *xy*. It is then possible to give a satisfactory interpretation of both the electronic absorption spectrum and the photoelectron spectrum. The compound crystallizes in the triclinic system with *a* = 8.442 (2) Å, *b* = 12.142 (2) Å, *c* = 14.196 (2) Å, α = 104.17 (2)°, β = 100.73 (1)°, γ = 84.67 (2)°, *V* = 1384.5 (8) Å³, and *Z* = 4. There are two crystallographically independent molecules which have essentially identical dimensions. The average values (over both molecules and assuming *D*_{2d} symmetry in each) of some important dimensions are the following: Mo–N, 1.926 (6) Å; N–C, 1.466 (15) Å; N–Mo–N, 109.5 (19)°; Mo–N–C, 124 (1)°, C–N–C, 110 (1)°.

Introduction

The purple, extremely volatile compound Mo(NMe₂)₄ was first isolated a number of years ago by Bradley and Chisholm,² who showed it to be a crystalline, diamagnetic compound and proposed a structure of *D*_{2d} symmetry on the basis of its diamagnetism and spectroscopic properties. Since then, a great deal of work has been done on the yellow, triply bonded Mo₂(NMe₂)₆ and its derivatives, and this has renewed our interest in having a more complete understanding of the mononuclear molecule, Mo(NMe₂)₄. One particular objective for characterizing this molecule structurally was to ascertain with certainty whether it could be used to obtain an estimate of the Mo–NMe₂ bond energy that would be required in order to deduce the Mo≡Mo bond energy from the heat of formation of Mo₂(NMe₂)₆. More generally, structure parameters were wanted as a basis for a more thorough study of the electronic structure of the molecule.

Procedures

The preparation and general properties of Mo(NMe₂)₄ have been described elsewhere.² It is an extremely oxygen- and moisture-sensitive compound and it was always handled in a N₂-filled glovebox. It is very volatile, subliming slowly at room temperature and 10⁻² Torr, and it melts at ca. 50 °C. Crystals of Mo(NMe₂)₄ were grown via sublimation in sealed, evacuated 8-mm glass tubes at room temperature. Selected crystals were wedged in thin-walled glass capillaries under N₂ and the capillaries were sealed with a small hand torch.

X-Ray Crystallography.³ An approximately spherical crystal of Mo(NMe₂)₄ measuring 0.32 mm in diameter was shown to be of good quality by ω scans of several intense reflections which had peak widths at half-height of ca. 0.2°. Cell constants and axial photographs indicated that the crystal belonged to the triclinic system with *a* = 8.442 (2) Å, *b* = 12.142 (2) Å, *c* = 14.196 (2) Å, α = 104.17 (2)°, β = 100.73 (1)°, γ = 84.67 (2)°, and *V* = 1384.5 (8) Å³. The observed

volume was consistent with that expected for *Z* = 4. The space group was assumed to be *P* $\bar{1}$; this was verified by the structure solution and refinement.

Data were collected at 4 °C on a Syntex *P* $\bar{1}$ autodiffractometer located in a cold room. The diffractometer was equipped with a monochromator and used Cu Kα radiation (λ 1.541 84 Å). The θ–2θ scan technique was used with scans ranging from 1.0° above to 1.0° below the calculated Kα₁, Kα₂ doublet, variable scan speeds ranging from 6.0 to 24.0°/min and a background to scan time ratio of 0.5. The intensities of three standard reflections were monitored frequently throughout data collection and showed no decrease in intensity. The integrated intensities of 3798 unique reflections having 0° < 2θ(Cu Kα) < 115° were collected.

A spherical absorption correction was applied to the data (μ = 79.0 cm⁻¹); the transmission coefficients ranged from 0.213 to 0.278 with an average of 0.250. The data were reduced to a set of relative |*F*_o|² values and the 2861 reflections having |*F*_o|² > 3σ(|*F*_o|²) were used in subsequent structure solution and refinement.

The structure was solved by conventional heavy-atom methods and refined to convergence using anisotropic thermal parameters for the Mo and N atoms and isotropic thermal parameters for the carbon atoms. Final unweighted and weighted residuals were *R*₁ = 0.056 and *R*₂ = 0.086, respectively. A value of 0.07 was used for *p* in the calculation of the weights.³ The end of an observation of unit weight was 1.993. The largest peaks in a final difference Fourier map were in regions where methyl group hydrogen atoms would be expected, but no attempt was made to include hydrogen atoms in the refined structure.

Molecular Orbital Calculations. The approximate but nonparameterized Hartree–Fock–Roothaan type MO Calculation commonly called the Fenske–Hall⁴ type was carried out using a program package and molybdenum wave functions kindly provided by Professor M. B. Hall of Texas A&M University. The atomic orbital coefficients and exponents of Richardson and co-workers were used,⁵ with double ζ functions for the metal d orbitals. Coefficients of 1.0 and exponents of 2.2 were chosen for the Mo 5s and 5p orbitals and these orbitals

Table I. Positional and Thermal Parameters and Their Estimated Standard Deviations^a

Atom	x	y	z	β_{11}	β_{22}	β_{33}	β_{12}	β_{13}	β_{23}
Mo(1)	0.29458 (7)	0.25234 (5)	0.52515 (4)	0.00991 (8)	0.00450 (5)	0.00466 (4)	-0.0015 (1)	0.00187 (9)	0.00179 (7)
Mo(2)	0.27909 (7)	0.25309 (5)	0.02916 (4)	0.01163 (10)	0.00576 (5)	0.00422 (4)	-0.0022 (1)	0.00251 (10)	0.00138 (7)
N(1)	0.1991 (8)	0.1496 (6)	0.4067 (5)	0.0156 (11)	0.0056 (5)	0.0047 (4)	-0.002 (1)	-0.0001 (11)	0.0026 (7)
N(2)	0.5268 (7)	0.2302 (6)	0.5522 (5)	0.0107 (9)	0.0063 (5)	0.0045 (3)	-0.001 (1)	0.0027 (9)	0.0024 (7)
N(3)	0.2399 (8)	0.4047 (6)	0.5104 (6)	0.0144 (11)	0.0048 (5)	0.0080 (5)	0.001 (1)	0.0015 (12)	0.0029 (8)
N(4)	0.2095 (7)	0.2251 (6)	0.6336 (5)	0.0104 (9)	0.0067 (5)	0.0047 (4)	-0.001 (1)	0.0029 (9)	0.0021 (7)
N(5)	0.1500 (8)	0.1301 (6)	-0.0522 (5)	0.0159 (11)	0.0068 (6)	0.0054 (4)	-0.002 (1)	0.0049 (10)	0.0016 (8)
N(6)	0.4263 (8)	0.2038 (6)	0.1338 (5)	0.0129 (10)	0.0087 (6)	0.0036 (3)	-0.002 (1)	0.0005 (10)	0.0026 (8)
N(7)	0.1333 (8)	0.3700 (6)	0.0884 (5)	0.0136 (10)	0.0061 (5)	0.0055 (4)	-0.001 (1)	0.0032 (10)	0.0011 (8)
N(8)	0.4065 (8)	0.3112 (6)	-0.0455 (5)	0.0110 (9)	0.0072 (6)	0.0056 (4)	-0.002 (1)	0.0018 (10)	0.0024 (8)

Atom	x	y	z	B, Å ²	Atom	x	y	z	B, Å ²
C(1)	0.249 (1)	0.0307 (9)	0.3797 (7)	5.1 (2)	C(9)	-0.007 (1)	0.1469 (9)	-0.1123 (7)	5.1 (2)
C(2)	0.036 (1)	0.1717 (9)	0.3544 (8)	5.4 (2)	C(10)	0.211 (1)	0.0127 (9)	-0.0793 (8)	5.9 (2)
C(3)	0.620 (1)	0.2761 (8)	0.6492 (7)	4.5 (2)	C(11)	0.560 (1)	0.2674 (10)	0.1922 (8)	6.1 (3)
C(4)	0.632 (1)	0.2025 (8)	0.4765 (7)	4.4 (2)	C(12)	0.385 (1)	0.1193 (9)	0.1831 (8)	5.7 (2)
C(5)	0.236 (1)	0.5052 (10)	0.5940 (9)	6.8 (3)	C(13)	0.167 (1)	0.4913 (10)	0.1282 (8)	5.9 (2)
C(6)	0.250 (1)	0.4425 (10)	0.4197 (8)	6.1 (3)	C(14)	-0.009 (1)	0.3452 (9)	0.1257 (8)	5.3 (2)
C(7)	0.268 (1)	0.1287 (9)	0.6790 (7)	5.1 (2)	C(15)	0.353 (1)	0.3949 (8)	-0.1051 (7)	4.9 (2)
C(8)	0.052 (1)	0.2662 (9)	0.6584 (7)	5.2 (2)	C(16)	0.560 (1)	0.2585 (8)	-0.0712 (7)	5.0 (2)

^a The form of the anisotropic thermal parameter is $\exp[-(\beta_{11}h^2 + \beta_{22}k^2 + \beta_{33}l^2 + \beta_{12}hk + \beta_{13}hl + \beta_{23}kl)]$.

Table II. Bond Distances, Å

Mo(1)-N(1)	1.921 (5)	Mo(2)-N(5)	1.934 (5)
Mo(1)-N(2)	1.932 (4)	Mo(2)-N(6)	1.928 (5)
Mo(1)-N(3)	1.917 (5)	Mo(2)-N(7)	1.927 (5)
Mo(1)-N(4)	1.924 (5)	Mo(2)-N(8)	1.927 (5)
N(1)-C(1)	1.443 (9)	N(5)-C(9)	1.461 (9)
N(1)-C(2)	1.471 (9)	N(5)-C(10)	1.454 (9)
N(2)-C(3)	1.460 (8)	N(6)-C(11)	1.435 (9)
N(2)-C(4)	1.476 (8)	N(6)-C(12)	1.474 (9)
N(3)-C(5)	1.483 (10)	N(7)-C(13)	1.476 (9)
N(3)-C(6)	1.488 (10)	N(7)-C(14)	1.484 (8)
N(4)-C(7)	1.474 (9)	N(8)-C(15)	1.465 (9)
N(4)-C(8)	1.449 (8)	N(8)-C(16)	1.457 (8)

^a Numbers in parentheses are estimated standard deviations in the least significant digits.

Table III. Bond Angles, deg

N(1)-Mo(1)-N(2)	112.5 (2)	N(5)-Mo(2)-N(6)	111.1 (2)
N(1)-Mo(1)-N(3)	108.2 (2)	N(5)-Mo(2)-N(7)	107.3 (2)
N(1)-Mo(1)-N(4)	108.1 (2)	N(5)-Mo(2)-N(8)	112.0 (2)
N(2)-Mo(1)-N(3)	109.1 (2)	N(6)-Mo(2)-N(7)	107.9 (2)
N(2)-Mo(1)-N(4)	108.0 (2)	N(6)-Mo(2)-N(8)	107.3 (2)
N(3)-Mo(1)-N(4)	111.0 (2)	N(7)-Mo(2)-N(8)	111.2 (2)
Mo(1)-N(1)-C(1)	123.5 (5)	Mo(2)-N(5)-C(9)	123.9 (5)
Mo(1)-N(1)-C(2)	122.1 (5)	Mo(2)-N(5)-C(10)	124.0 (5)
C(1)-N(1)-C(2)	111.1 (6)	C(9)-N(5)-C(10)	110.7 (6)
Mo(1)-N(2)-C(3)	121.8 (4)	Mo(2)-N(6)-C(11)	123.7 (5)
Mo(1)-N(2)-C(4)	124.7 (4)	Mo(2)-N(6)-C(12)	122.7 (5)
C(3)-N(2)-C(4)	110.5 (5)	C(11)-N(6)-C(12)	110.9 (6)
Mo(1)-N(3)-C(5)	124.1 (5)	Mo(2)-N(7)-C(13)	126.0 (4)
Mo(1)-N(3)-C(6)	123.5 (5)	Mo(2)-N(7)-C(14)	123.1 (4)
C(5)-N(3)-C(6)	109.6 (6)	C(13)-N(7)-C(14)	109.0 (5)
Mo(1)-N(4)-C(7)	122.5 (4)	Mo(2)-N(8)-C(15)	126.6 (4)
Mo(1)-N(4)-C(8)	125.2 (5)	Mo(2)-N(8)-C(16)	124.1 (5)
C(7)-N(4)-C(8)	109.2 (5)	C(15)-N(8)-C(16)	107.8 (5)

^a Numbers in parentheses are estimated standard deviations in the least significant digits.

were normalized with respect to the inner shell s and p orbitals. Calculations were carried out using Mo(+1) and Mo(+2) orbital functions, and the latter yielded a final net Mo atomic charge (d orbitals only) more consistent with the chosen "oxidation state", although no major differences were noted between the two sets of results. A preliminary calculation carried out on lone $\cdot\text{NMe}_2$ ligands allowed us to formulate the final $\text{Mo}(\text{NMe}_2)_4$ MO's in terms of the ligand MO's, rather than AO's of ligand atoms. The only ligand orbitals interacting appreciably with the metal atom were the two highest ligand orbitals, namely, the lone pair $p\pi$ orbital perpendicular to the NC_2 plane and the nitrogen σ orbital lying in the NC_2 plane.

Atomic coordinates were based on average molecular dimensions taken from the crystal structure averaged according to D_{2d} symmetry.

Table IV. Average Distances (Å) and Angles (deg) in $\text{Mo}(\text{NMe}_2)_4$

Atoms	n^a	Average ^b	Range
Distances			
Mo-N	8	1.926 (6)	1.917 (5)-1.934 (5)
N-C	16	1.466 (15)	1.443 (9)-1.488 (10)
Angles			
N-Mo-N	12	109.5 (19)	107.3 (2)-112.5 (2)
Mo-N-C	16	124 (1)	121.8 (4)-126.6 (4)
C-N-C	8	110 (1)	107.8 (5)-111.1 (6)

^a n is the number of crystallographically independent values averaged. ^b Numbers in parentheses are the standard deviation of the mean.

Table V. Dihedral Angles between Planes in Molecules I and II

Molecule I		Molecule II	
Plane no.	Atoms	Plane no.	Atoms
1	N(1)-Mo(1)-N(4)	7	N(5)-Mo(2)-N(8)
2	N(2)-Mo(1)-N(3)	8	N(6)-Mo(2)-N(7)
3	C(1)-N(1)-C(2)	9	C(9)-N(5)-C(10)
4	C(7)-N(4)-C(8)	10	C(15)-N(8)-C(16)
5	C(3)-N(2)-C(4)	11	C(11)-N(6)-C(12)
6	C(5)-N(3)-C(6)	12	C(13)-N(7)-C(14)

Planes	Angle, deg	Planes	Angle, deg
1-2	93	7-8	93
1-3	91	7-9	89
1-4	89	7-10	89
2-5	87	8-11	93
2-6	88	8-12	89

Results

Structural. $\text{Mo}(\text{NMe}_2)_4$ crystals are formed from discrete mononuclear molecules. There are two crystallographically independent but essentially identical molecules per asymmetric unit. Final atomic positional and thermal parameters, bond distances, and angles are given in Tables I, II, and III, respectively. Two ORTEP views of molecule I are given in Figure 1. The atom labeling scheme used for molecule II parallels that used for molecule I and is obtained therefrom by replacing Mo(1), N(1)-N(4), and C(1)-C(8) by Mo(2), N(5)-N(8), and C(9)-C(16), respectively. Average bond distances and angles are given in Table IV and the dihedral angles between planes which are important in defining the molecular symmetry are given in Table V.

Each molybdenum atom is coordinated to four dimethyl-amido ligands. The MoN_4 moieties have nearly perfect T_d

Table VI. Pertinent Eigenvalues and Eigenfunctions; Percentage Contributions of Metal AO's and Ligand Orbitals to MO's

MO	Energy, eV	Metal orbitals					Ligand orbitals			
		$4d_{z^2}$	$4d_{x^2-y^2}$	$4d_{xy}$	$4d_{xz}/4d_{yz}$	5s	5p _x /5p _y	5p _z	σ	π
3b ₂	-0.02	0	0	59	0	0	0	24	12	4
3e	-0.88	0	0	0	59	0	27	0	6	7
3a ₁	-2.63	72	0	0	0	0	0	0	1	27
1b ₁	-5.32	0	97	0	0	0	0	0	0	0
2e	-9.82	0	0	0	3	0	1	0	6	91
2b ₂	-9.93	0	0	2	0	0	0	4	0	94
2a ₁	-11.45	28	0	0	0	0	0	0	0	71
1a ₁	-14.80	0	0	0	0	21	0	0	70	0
1e	-16.00	0	0	0	22	0	6	0	67	2
1b ₂	-16.36	0	0	25	0	0	0	5	69	0

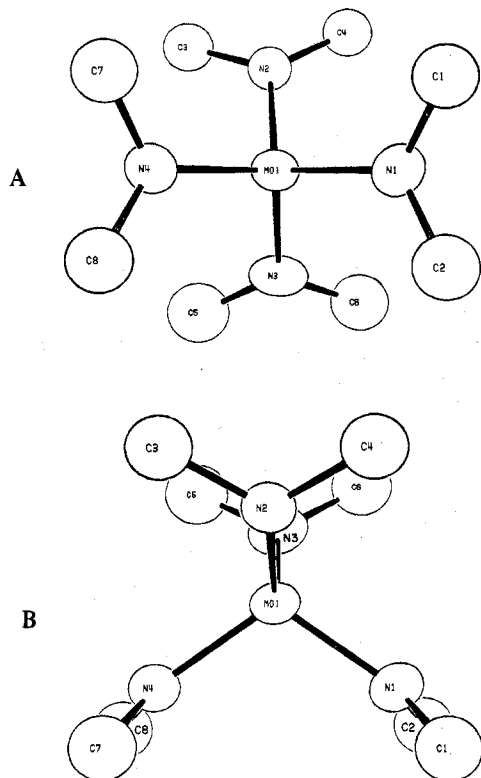


Figure 1. Two ORTEP views of molecule I using 50% probability ellipsoids and showing the atom labeling scheme. Molecule II is essentially identical with molecule I. View B is rotated 90° about the horizontal axis of view A.

symmetry and the Mo-NC₂ moieties are essentially planar, with the NC₂ planes oriented so as to give the molecule practically exact D_{2d} symmetry. Inspection of the dihedral angles listed in Table V, which would be 90° if the molecule had exact D_{2d} symmetry, will show how slight are the deviations from exact D_{2d} symmetry. The two ORTEP drawings in Figure 1 are views of the molecule taken almost directly down and almost perpendicular to the unique twofold axis of the D_{2d} point group.

MO Calculations. The results of the calculations are displayed in Figure 2. Energies of those filled and empty orbitals which are pertinent to a discussion of the bonding in Mo(NMe₂)₄ are shown in Table VI. Also listed are the percent contributions of the Mo atomic orbitals and the σ and π ligand orbitals to the overall MO's. Figure 2 gives a diagrammatic representation of the results obtained using the d functions for Mo²⁺.

Discussion

A molecular structure of D_{2d} symmetry, based on a "tetrahedral" arrangement of the nitrogen atoms about the molybdenum atom, as earlier suggested,² has been found. A

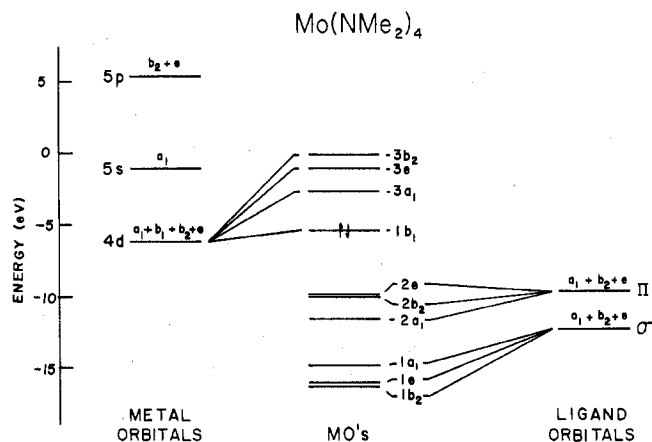


Figure 2. A molecular orbital diagram for Mo(NMe₂)₄ showing the orbitals pertinent to MoN₄ bonding. The highest occupied MO is marked with arrows. The lines indicate the predominant π character of the MO's.

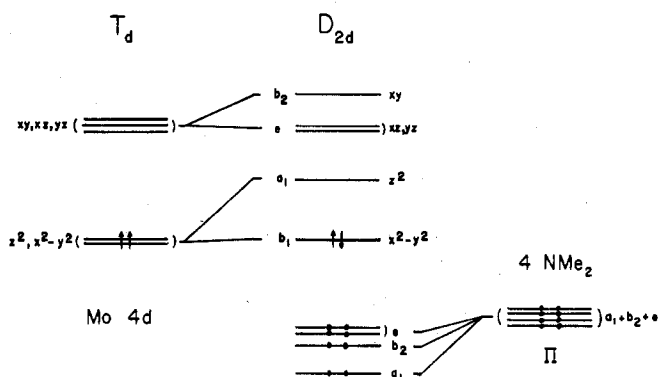


Figure 3. The qualitative orbital splitting diagrams for a d² complex under tetrahedral (T_d) symmetry and after introduction of a pronounced D_{2d} component arising from the presence of the lone pair π orbitals on the ligands.

truly tetrahedral Mo^{IV}L₄ complex would be expected to have two unpaired "d" electrons, occupying a degenerate orbital of e symmetry, whereas Mo(NMe₂)₄ is diamagnetic. Because of interaction of the lone pair orbitals of the nitrogen atoms with the metal d orbitals there is a lifting of the degeneracy mentioned with the result that the two "d" electrons become paired. The qualitative picture is summarized in Figure 3.

The four lone pair orbitals on the nitrogen atoms span the representations a₁, b₂, and e in D_{2d} symmetry and their interactions with the metal d orbitals cause all of the latter except d_{x²-y²} to rise in energy, thus isolating this orbital. The cause of the splitting apart of the d_{z²} and d_{x²-y²} orbitals is easily visualized in terms of the π interaction shown in Figure 4, which raises the energy of the d_{z²} orbital. Qualitatively the direction of the splitting is predictable unambiguously since

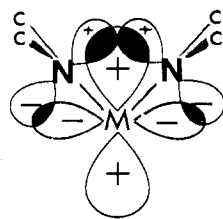


Figure 4. π overlap of the metal $d_{x^2-y^2}$ orbital with nitrogen p_{π} orbitals. Two more such overlaps occur with the lower part of the $d_{x^2-y^2}$ orbital in the plane perpendicular to the page.

the $d_{x^2-y^2}$ orbital has b_1 symmetry and there is no possibility of its interacting with any of the nitrogen lone-pair orbitals nor with any of the Mo–N σ orbitals since neither of these sets includes a combination of b_1 symmetry. The splitting of the xz , yz , xy set so that the $b_2(xy)$ orbital goes above the (xz , yz) orbital also follows qualitatively from the relative overlap with the b_2 and e symmetry combinations of the nitrogen lone-pair orbitals; the b_2 overlap is distinctly greater than the e overlap.

Although this picture is qualitatively unambiguous and furnishes sound guidance to assigning both the electronic absorption spectrum and the photoelectron spectrum (PES), we considered it worthwhile to carry out a quantitative, though approximate, analysis of the electronic structure as well. This was done using the Fenske–Hall method for simplifying the Hartree–Fock–Roothaan type calculation. The results of this are listed in Table VI and shown in Figure 2. The results presented are those obtained when metal orbitals appropriate to Mo^{2+} were used as input. The final charges were +1.25 for the Mo atom as a whole and +1.78 for the d orbitals. Another calculation using metal orbitals corresponding to Mo^+ give a final total metal charge of +0.96 and a d-orbital charge of +1.56; because of the greater discrepancy between calculated charges and the value used to select the orbital radial functions this was considered a less realistic calculation than the first one, although the level order was qualitatively the same.

It is clear that the Fenske–Hall calculation affords an ordering of orbitals that is the same as that (Figure 3) anticipated from qualitative overlap considerations. Using Table VI and Figure 2 we now proceed to consider assignments for the PES and electronic absorption spectra. The PES, which will be reported in detail elsewhere as part of a broad study of $\text{M}(\text{NR}_2)_n$ compounds by Chisholm and Cowley, has the following absorption bands: IE_1 5.30 eV (sharp); IE_2 7.34 eV (broad); IE_3 7.70 eV (sharp); IE_4 9.01 eV (broad); IE_5 10.7 eV (very broad). The IE_5 peak is then followed by a series of broad, overlapping absorptions from about 11.5 to 15 eV, which doubtless correspond to ionizations of N–C and C–H bonding electrons.

The sharp peak at 5.30 eV, IE_1 , may be assigned to ionization of the b_1 level, the essentially pure $d_{x^2-y^2}$ orbital. The next two peaks, IE_2 and IE_3 , would correspond to the 2e and

$2b_2$ levels and IE_4 to the $2a_1$ level. The observed spacings and the calculated orbital separations agree only approximately, but considering that relaxation effects are being neglected, the general similarity is satisfying. The sharpness of IE_1 is consistent with the nondegenerate, nonbonding character of the $1b_1$ level. The breadth of IE_2 can be attributed to a Jahn–Teller effect. The increasing breadth of the IE_4 and IE_5 peaks is consistent with their increasingly bonding character. It is possible and even likely that the very broad IE_5 represents unresolved ionizations of the $1a_1$, $1e$, and $1b_2$ levels.

The electronic absorption spectrum cannot be completely assigned with certainty, but there are no serious difficulties. The lowest reported shoulder at $10\,500\text{ cm}^{-1}$ with $\epsilon \approx 30$ can be assigned with little doubt to the $1b_1 \rightarrow 3a_1$ (${}^1B_1 \leftarrow {}^1A_1$) transition which is orbitally forbidden. The $1b_1 \rightarrow 3e$ (${}^1E \leftarrow {}^1A_1$) transition, orbitally allowed, should be next and we suggest this assignment for the next shoulder at $14\,300\text{ cm}^{-1}$ with $\epsilon \approx 300$. The two strong ($\epsilon \approx 1000$) peaks at $19\,600$ and $21\,700\text{ cm}^{-1}$ are probably charge-transfer bands ($2e$ and $2b_2$ to $3a_1$ transitions) which cover the $1b_1 \rightarrow 3b_2$ (${}^1A_2 \leftarrow {}^1A_1$) “d–d” transition expected a little above the ${}^1E \leftarrow {}^1A_1$, “d–d” transition.

Finally, we return to our point of departure in studying this molecule in detail. As already stated, this was to determine whether it could serve as a vehicle for estimating the Mo–N bond energy in $\text{Mo}_2(\text{NMe}_2)_6$.⁶ Qualitatively it is satisfactory, since it has four equivalent Mo–N bonds. There is also a very close quantitative similarity of the Mo–NMe₂ units in the two molecules. The N–C distances have average values of $1.47 \pm 0.02\text{ \AA}$ in both molecules and the mean C–N–C angles in the essentially planar Mo–NC₂ units are also indistinguishable in the two cases, viz., $110 \pm 1^\circ$. The only pertinent difference is in the Mo–N distances, which is not unexpected in view of the different formal oxidation numbers. Thus, the mean Mo–N distance in $\text{Mo}(\text{NMe}_2)_4$ is $1.926(6)\text{ \AA}$, while in $\text{Mo}_2(\text{NMe}_2)_6$ we previously found $1.98 \pm 0.01\text{ \AA}$.

Acknowledgment. We thank the National Science Foundation for support. We are grateful to Professor Alan Cowley for allowing us to cite his PES data and to Mr. J. W. Chinn and Professor M. B. Hall for their guidance in the use of the Fenske–Hall program package.

Registry No. $\text{Mo}(\text{NMe}_2)_4$, 33851-46-6.

Supplementary Material Available: A table of observed and calculated structure factors (13 pages). Ordering information is given on any current masthead page.

References and Notes

- (1) (a) Princeton University. (b) Texas A&M University.
- (2) D. C. Bradley and M. H. Chisholm, *J. Chem. Soc. A*, 2741 (1971).
- (3) All crystallographic computing was carried out on a PDP 11/45 computer owned by Molecular Structure Corporation, College Station, Texas, using the Enraf-Nonius structure determination package.
- (4) M. B. Hall and R. F. Fenske, *Inorg. Chem.*, **11**, 768 (1972).
- (5) J. W. Richardson, M. J. Blackman, and J. E. Ranochak, *J. Chem. Phys.*, **58**, 3010 (1973).
- (6) M. H. Chisholm, F. A. Cotton, B. A. Frenz, W. W. Reichert, L. W. Shive, and B. R. Stultis, *J. Am. Chem. Soc.*, **98**, 4469 (1976).